Impact of Adjacent/Overlapping Communication Waveform Design within a Radar Spectrum Sharing Context

Justin G. Metcalf
School of Electrical and
Computer Engineering
Advanced Radar Research Center
University of Oklahoma
Norman, Oklahoma

Cenk Sahin,
Patrick McCormick
AFRL Sensors Directorate
Dayton, Ohio

Shannon D. Blunt
Radar Systems Lab
University of Kansas
Lawrence, Kansas

***Abstract*—We consider the design of spectrum sharing communication waveforms that may partially overlap spectrally with a pulse-Doppler radar yet maintain a low, predictable level of interference with radar operation. This is in contrast to traditional communication waveforms, which can interfere with radar operation despite having a negative interference-to-noise ratio. A new communication symbol design is derived as an improvement on previously developed subspace projection based designs. The new design provides a significant reduction in interference to radar operation while maintaining comparable symbol error rate performance to the previous methods.**

I. Introduction

The congestion of the electromagnetic spectrum has motivated significant research efforts into techniques for spectrum sharing between radar and communications systems. One common approach is to consider the radar as a secondary user that must operate in a congested spectrum where communications users have priority [1], [2]. In contrast we consider a spectrum sharing scenario where a communication system is a secondary user operating physically near a primary radar user. As a secondary user, the communication waveforms must minimize their interference to the radar operation while still being robust to interference from the radar. As a first step, we will propose a framework for the design of physical layer communication waveforms based on a signal-to-interference metric.

Specifically, consider the design of communication waveforms that must operate spectrally adjacent to a high power search radar, or even with partial spectral overlap. A possible motivating application is a communication system broadcasting data to a radar. Under this scenario the radar may receive and demodulate the communication symbols by simply oversampling the spectrum relative to the bandwidth of the radar waveform. Future work will extend to the more general case where the communication system is merely operating near (in a physical and spectral sense) a search radar.

While the Central Limit Theorem has been invoked to model interference due to communication signals at a radar as complex Gaussian interference [3], experimentation and simulation has noted impact to radar performance at negative interference-to-noise ratios (INR) [4], [5]. A consequence of this interference is an increased bias to a constant false alarm rate (CFAR) detector, causing a reduction in detection sensitivity. By definition, if the performance of CFAR detector is impacted by interference with a power less than the noise floor, it cannot be considered to be distributed as complex Gaussian. Therefore, the symbol design presented here is motivated by a desire to minimize interference at the radar as measured by both the signal-to-interference ratio (SIR) at the output of the radar matched filter and the statistics of the residue after pulse-Doppler processing. These results have been shown for a multitude of traditional communication waveforms, including phase shift keying (PSK), quadrature amplitude modulation (QAM), and orthogonal frequency division multiplexing (OFDM) [4], [5].

A similar concept was recently proposed [6] where a waterfilled OFDM communications waveform was transmitted within the passband and spectral rolloff of a simple search radar using a tapered transmit spectrum. However, in contrast to [6], we consider a pulse compression search radar using pulse-Doppler processing. As will be shown in Section III we also use a form of waterfilling, but in a subspace domain rather than the frequency domain. However, in a follow-on journal article the proposed approach will be compared against an OFDM approach.

II. Signal Model

Assume that a radar transmits a continuous pulse compression waveform $s(t)$ sampled at complex baseband with 3 dB bandwidth B_r and corresponding radar code chip time $T_r \approx \frac{1}{B_r}$. The radar pulse is T_p seconds long,and therefore has a time-bandwidth product of $N = \frac{T_p}{T_r} = T_p B_r$. If the received signal is oversampled by a factor of M, the radar waveform can be represented by the discrete values $\mathbf{s} = [s_0, \ldots, s_{NM-1}]^T$. Note that increasing the oversampling factor M corresponds with expanding the bandwidth sampled by the radar receiver, B_s. As such, provided the receiver is capable of expanding its bandwidth (e.g. bandpass/anti-aliasing filters permitting) will naturally admit frequency content spectrally adjacent to the radar waveform.

Consider the design a set of K communication symbols $c_k(t), k = 1, ...K$, allowing for the embedding of $log_2(K)$ bits of information per transmitted symbol (assuming no coding). It is assumed that the time extent of a single communication symbol is equal to that of the radar pulse, and the symbol chip time is sampled at a rate of $T_c = \frac{T_r}{M}$. Therefore, the communications symbols are designed to occupy a spectral extent $B_c = MB_r$. Previous work in [7] examined the construction of direct sequence spread spectrum (DSSS) spreading codes in the presence of additive colored interference. Here we will extend the formulation proposed in [7] by assuming the radar waveform to be the source of colored interference.

The continuous time received signal at the communication receiver for the kth symbol is represented as

$$r(t) = \alpha c_k(t) + s(t) * x(t) + u(t), \tag{1}$$

where α is the complex fading coefficient of the communication symbol, $u(t)$ is thermal additive white Gaussian noise, and $x(t)$ is a random process representing the channel profile between the radar transmitter and the communication receiver. The channel profile may consist of radar backscatter (i.e. clutter), forward scatter, and/or reflections from moving targets.

Subsequently, the sampled radar waveform and the k^{th} communication symbol are given as the $NM \times 1$ vectors $\mathbf{s}$ and $\mathbf{c}_k$, respectively. The sampled complex baseband receive signal of the kth symbol is then

$$\mathbf{r}_\ell = \alpha \mathbf{c}_k + \mathbf{S}\mathbf{x} + \mathbf{u}, \tag{2}$$

where the $2NM-1 \times 1$ vector $\mathbf{x}$ is the sampled channel profile and the discrete convolution matrix $\mathbf{S}$ is the Toeplitz matrix

$$\mathbf{S} = \begin{bmatrix} s_{NM-1} & s_{NM-2} & \cdots & s_0 & 0 & \cdots & 0 \\ 0 & s_{NM-1} & \cdots & s_1 & s_0 & \cdots & 0 \\ \vdots & \vdots & \ddots & \vdots & \vdots & \ddots & \vdots \\ 0 & 0 & \cdots & s_{NM-1} & s_{NM-2} & \cdots & s_0 \end{bmatrix}. \tag{3}$$

To determine the transmitted symbol the received signal is filtered by the communication receiver with a filter bank, where the filter corresponding to the k^{th} symbol is denoted as $\mathbf{w}_k^H$. The output of the filter corresponding to the transmitted signal is then

$$y_\ell = \mathbf{w}_k^H \mathbf{r}_\ell = \alpha \mathbf{w}_k^H \mathbf{c}_k + \mathbf{w}_k^H \mathbf{S}\mathbf{x} + \mathbf{w}_k^H \mathbf{u}. \tag{4}$$

The output signal-to-interference-plus-noise ratio (SINR) after filtering is found from the components of the magnitude squared filtered response as

$$\begin{aligned} E\left[|y_\ell|^2\right] &= E\left[\left((\alpha \mathbf{c}_k)^H \mathbf{w}_k \mathbf{w}_k^H (\alpha b_\ell \mathbf{c}_k)\right)\right] \\ &+ E\left[\left((\mathbf{S}\mathbf{x})^H \mathbf{w}_k \mathbf{w}_k^H (\mathbf{S}\mathbf{x})\right)\right] \\ &+ E\left[\left(\mathbf{u}^H \mathbf{w}_k \mathbf{w}_k^H \mathbf{u}\right)\right] \\ &= S + R + N. \end{aligned} \tag{5}$$

Under the assumption that the samples of the channel profile process are independent, identically distributed zero-mean complex random variables, the filtered interference power from (5) is

$$\begin{aligned} R &= E\left[\left((\mathbf{S}\mathbf{x})^H \mathbf{w}_k \mathbf{w}_k^H (\mathbf{S}\mathbf{x})\right)\right] \\ &= E\left[\mathbf{w}_k^H \mathbf{S}\mathbf{x}\mathbf{x}^H \mathbf{S}^H \mathbf{w}_k\right] \\ &= \mathbf{w}_k^H \mathbf{S} E\left[\mathbf{x}\mathbf{x}^H\right] \mathbf{S}^H \mathbf{w}_k \\ &= \sigma_x^2 \mathbf{w}_k^H \mathbf{S}\mathbf{S}^H \mathbf{w}_k \end{aligned} \tag{6}$$

It is well-known that the matched filter (i.e. $\mathbf{w}_k = \mathbf{c}_k$) will maximize signal-to-noise ratio (SNR) for the received signal. Therefore, under the assumption of matched filtered receive processing and unit-normed codes (i.e. $\mathbf{c}_k^H \mathbf{c}_k = 1$), the SINR of the filtered response can be found from the components of (5) as

$$\begin{aligned} SINR_o &= \frac{S}{R+N} \\ &= \frac{|\alpha \mathbf{w}_k^H \mathbf{c}_k|^2}{\sigma_x^2 \mathbf{w}_k^H \mathbf{S}\mathbf{S}^H \mathbf{w}_k + \sigma_u^2 \mathbf{w}_k^H \mathbf{w}_k} \\ &= \frac{|\alpha|^2}{\sigma_x^2 \mathbf{c}_k^H \mathbf{S}\mathbf{S}^H \mathbf{c}_k + \sigma_u^2} \end{aligned} \tag{7}$$

Thus the spreading codes may be used as communication symbols themselves. Consequently, consider the SIR of the communications symbol to the radar interference,

$$SIR_o = \frac{S}{R} = \frac{|\alpha|^2}{\sigma_x^2 \mathbf{c}_k^H \mathbf{S}\mathbf{S}^H \mathbf{c}_k}. \tag{8}$$

In order to maximize communication performance in the presence of colored interference from the radar, we heuristically consider the problem of designing communication symbols to minimize the overlap with the interference term in the denominator of (8). A formal optimization of (8) will be examined in future work. As was noted in [7] the interference may be expressed as an eigendecomposition

$$\mathbf{S}\mathbf{S}^H = \mathbf{V}\mathbf{\Lambda}\mathbf{V}^H, \tag{9}$$

where the columns of $\mathbf{V}$ are the collection of orthonormal eigenvectors and the non-zero entries of the diagonal matrix $\mathbf{\Lambda}$ are the descending eigenvalues corresponding to each eigenvector. Therefore, the eigenvectors $\mathbf{v}$ associated with the smallest eigenvalues may be used as waveforms.

While starting from a different model, the same conclusion was reached for a communications symbol design for embedding communication symbols in radar clutter [8], [9]. However, it was noted that the so-called eigenvectors-as-waveforms, while the highest performing design in noise, were highly sensitive to multipath [10]. Therefore, several other communication symbol designs were developed and analyzed [8], [9], [11]–[16]. As these symbol designs were developed from an identical mathematical model, we will examine their performance as spectrum sharing waveforms.

III. SYMBOL DESIGNS

By allowing the bandwidth of the communication symbols to expand while maintaining the same center frequency results in a wideband communications waveform *centered* around the spectrum allocated to the radar. Therefore, as a baseline, we will consider a traditional direct sequence spread spectrum (DSSS) symbol design composed of complex Gaussian distributed values. We will then present three competing symbol designs to improve on the DSSS approach. The general solution consists of a base spreading code and a subspace projection matrix derived from the eigendecomposition of (9).

A. Direct Sequence Spread Spectrum Symbol Design

The direct sequence spread spectrum (DSSS) symbol design is simply a set of K unit-normed, length $NM \times 1$ vectors $\mathbf{b}_1, ..., \mathbf{b}_k, ..., \mathbf{b}_K$ where the individual chip values of each vector are drawn from the distribution $b_{k,i} \sim \mathcal{CG}(0,1)$. For comparison's sake, the symbols are then unit-normed by multiplying by a the energy normalization factor γ_{DSSS}.

$$\begin{aligned} \mathbf{c}_{\text{DSSS},k} &= \gamma_{\text{DSSS}} \mathbf{b}_k \\ &\approx \frac{1}{NM} \mathbf{b}_k \end{aligned} \tag{10}$$

B. Dominant Projection Symbol Design

As previously noted, a solution to spreading code design was presented in [7] by using the individual eigenvectors of (9) as spreading codes (communication symbols in our case). However, an alternate solution was presented in [12], [17]. Consider the partition of the eigenspace into "dominant" and "non-dominant" eigenvectors. This partition is expressed as

$$\mathbf{V}\mathbf{\Lambda}\mathbf{V}^H = \left[\begin{array}{c|c} \mathbf{V}_{\text{D}} & \mathbf{V}_{\text{ND}} \end{array}\right] \left[\begin{array}{c|c} \mathbf{\Lambda}_{\text{D}} & \mathbf{0} \\ \hline \mathbf{0} & \mathbf{\Lambda}_{\text{ND}} \end{array}\right] \left[\begin{array}{c} \mathbf{V}_{\text{D}}^H \\ \hline \mathbf{V}_{\text{ND}}^H \end{array}\right]. \tag{11}$$

Ostensibly the set of $m = N$ dominant eigenvectors span the space occupied by the interference term. Therefore, a projection matrix may be formed to project away from the interference

$$\begin{aligned} \mathbf{A} &= \mathbf{I} - \mathbf{V}_{\text{D},m} \mathbf{V}_{\text{D},m}^H \\ &= \mathbf{V}_{\text{ND},m} \mathbf{V}_{\text{ND},m}^H. \end{aligned} \tag{12}$$

Subsequently, in the donminant projection formed by projecting *away* from these dominant eigenvectors. By using a subspace as a whole, it was shown that the resultant symbols were robust to multipath and estimation errors [14], [17]. The k^{th} dominant projection (DP) communication symbol is then formed as

$$\begin{aligned} \mathbf{c}_{\text{DP},k} &= \beta_{\text{DP},m}^{1/2} \mathbf{A} \mathbf{b}_k \\ &= \beta_{\text{DP},m}^{1/2} \mathbf{V}_{\text{ND},m} \mathbf{V}_{\text{ND},m}^H \ \mathbf{b}_k, \end{aligned} \tag{13}$$

where the unit-norm enforcing scaling factor is found as

$$\beta_{\text{DP},m} \approx \frac{NM}{NM - m}. \tag{14}$$

Note that for this symbol design a parameter m must be chosen to define the dominant subspace (i.e. the eigenvectors associated with the m largest eigenvalues). This "dial" permits tuning the amount of overlap between the radar waveform (where $m = 0$ is a full overlap and $m = NM - 1$ is minimal overlap) and the communication waveform.

C. Shaped Dominant Projection Symbol Design

A modification to the dominant projection approach was proposed in [15], where the projected symbols were scaled by their corresponding eigenvalues as

$$\mathbf{c}_{\text{SDP},k} = \beta_{\text{SDP}}^{1/2} \mathbf{V}_{\text{ND},m} \mathbf{\Lambda}_{\text{ND},m}^{1/2} \mathbf{V}_{\text{ND},m}^H \mathbf{b}_k, \tag{15}$$

with corresponding energy normalization factor

$$\beta_{\text{SDP}} \approx \frac{NM}{\text{tr}\left\{\mathbf{\Lambda}_{\text{ND},m}\right\}}. \tag{16}$$

This approach was called the shaped dominant projection (SDP) symbol design, and was proposed to force the communication symbols to better follow the spectral rolloff of the radar clutter.

D. Inverse Shaped Dominant Projection Symbol Design

Taking inspiration from the SDP symbol design, here we propose an inverse SDP symbol design, where in a waterfilling approach (similar to that of [6]) we scale the projection by the inverse of the associated eigenvalues. Formally, we define the k^{th} ISDP symbol as

$$\mathbf{c}_{\text{ISDP},k} = \beta_{\text{ISDP}}^{1/2} \mathbf{V}_{\text{ND},m} \mathbf{\Lambda}_{\text{ND},m}^{-1/2} \mathbf{V}_{\text{ND},m}^H \mathbf{b}_k, \tag{17}$$

with energy normalization factor

$$\beta_{\text{ISDP}} = \frac{NM}{\text{tr}\left\{\mathbf{\Lambda}_{\text{ND},m}^{-1}\right\}}. \tag{18}$$

E. Comments on Symbol Design Methods

In contrast to the DP and SDP symbol designs, the ISDP symbol design will allocate more power to the subspace outside of the dominant eigenvalues - in other words the guard band. The subspace projection used in (13), (15), and (17) projects the symbols from a NM dimensional space into a $NM - m$ dimensional subspace. Therefore, there is naturally a tradeoff between the number of symbols K that may be embedded in the $NM - m$ dimensional subspace and the separability of the symbols. In the previous work of [8], [9], [11]–[15] very small constellation sizes were chosen, where $K = 4$ or 8 when $M = 64$ and $N = 2$. In other words, there were significantly more degrees of freedom than constellation points. These symbols were designed to be easily separable at the cost of lower data rates (2 and 3 bits/symbol, respectively). In contrast, we consider the number of symbols transmitted to be equal to $NM - m$ to increase the data rate and improve the spectrum sharing performance.

The ability to define the dominant subspace according to operating requirements provides flexibility to retain dimensionality for constellation points as a function of the output

SIR or SINR. Past work chose m as a function of processing gain (i.e. ratio of output SINR to input SINR) for the DP and SDP symbol designs [14]–[16]. However, in a spectrum sharing context the impact to the radar will also need to be considered. Therefore, in future work the SINR at the radar will be incorporated into the processing gain equation to derive the optimal value of m for spectrum sharing. It is expected that synchronization and equalization will be more challenging for the ISDP symbols as compared to OFDM, as is the case with most spread spectrum symbol designs.

While the complex Gaussian code values used here are more challenging to implement (both from a processing and a hardware perspective) than traditional Walsh-Hadamard, Gold, or other binary pseudo-random codes, they are chosen here to improve co-existence with the radar. Specifically, by choosing a spectrally white base for the symbol design, it is expected that the output of radar pulse-Doppler processing will be complex Gaussian interference, allowing for *predictable* impact on radar performance. An initial analysis of this hypothesis is presented in Section IV-B, but more work is needed to make a definitive conclusion.

IV. Simulation Results

An initial set of communication symbols were implemented using the designs given in Section III. The radar waveform is a $10\mu s$ linear frequency modulated (LFM) waveform with 10 MHz of bandwidth, yielding a time-bandwidth product of $N = 100$. The communication symbols were designed with an oversample factor of $M = 2$, yielding 20 MHz of communication bandwidth. Three sets of DP, SDP, and ISDP symbols were generated using dominant subspace dimensionalities of $m = [50, 100]$, corresponding to $m = [N/2, N]$. All symbols used the DSSS symbols as a baseline prior to projection. In a key departure from previous work, the number of symbols for each set was $K = NM - m$, or $K = [150, 100]$, respectively. This was done to maximize the data rate at the cost of interference and noise tolerance. All communication symbols and the radar waveform were normalized to possess the same pulse length and unit energy. The performance of the spectrum sharing communication symbols were analyzed in three contexts: spectral content, impact to the radar, and symbol error rate.

A. Average Spectral Content of Symbols

First, the average spectrum of each symbol design was compared as a function of subspace dimensionality. In Figure 1 the DP, SDP, and ISDP communications symbols are projected away from the subspace spanned by the $m = N/2 = 50$ dominant eigenvectors. Inside the radar passband the DP and ISDP symbols largely overlap, but the impact of the shaping of the SDP symbols is clear in spectral rolloff region. Meanwhile, the impact of the waterfilling approach used by ISDP symbols manifests in higher power allocations on the outer frequencies.

For the $m = N = 100$ case shown in Figure 2 the poor spectrum sharing performance of the SDP waveforms is clear.

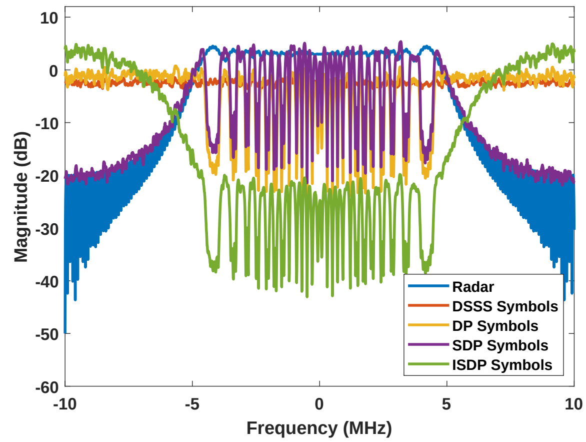

Fig. 1. Spectral content for $m = N/2$.

There is significantly more communication symbol energy allocated within the radar passband, and the normalization further causes overlap on the edges of the radar passband near the "peaks" from the largest eigenvalues in the non-dominant subspace. However, the ISDP symbols achieve improved suppression within the radar passband.

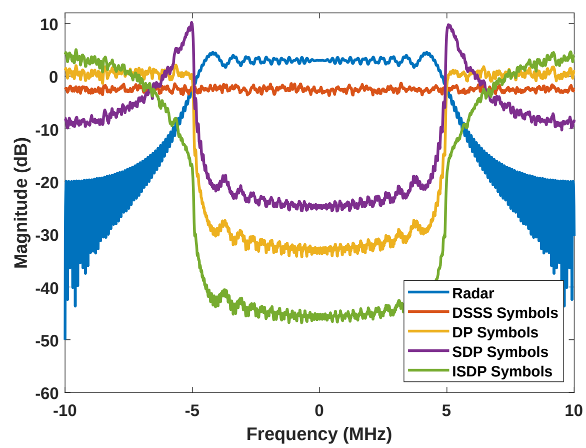

Fig. 2. Spectral content for $m = N$.

B. Impact at Radar

Next we examine the impact at the radar using two different metrics. First, Figures 3 and 4 show the average output of the radar matched filter for both the radar waveform (i.e. the pulse compression response) and the communication symbols.

Figure 3 shows the response for symbols designed with $m = N/2 = 50$. Note that while the DP symbols provide a slight improvement in cross-correlation as compared to the full dimensional DSSS symbols, the correlation induced by the shaping of the SDP symbols results in a cross-correlation response of greater magnitude than the DSSS symbols. This increased response is despite the symbols being projected away from half of the subspace spanned by the radar waveform. In contrast, the shaping of the ISDP symbols provides more than 45 dB of interference suppression simply from the radar matched filter. Therefore, from an SIR perspective - where the signal is a radar return and the interference is the communication waveform - this symbol may be received at the radar above the noise floor and have very little impact on radar performance.

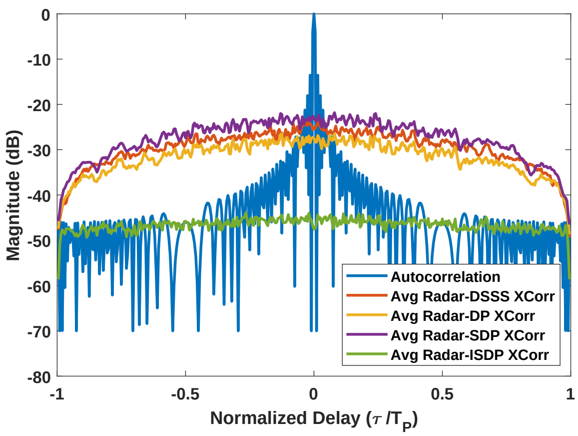

Fig. 3. Radar matched filter output for $m = N/2$.

In Figure 4 the dominant subspace is chosen to be $m = N = 100$. The DP symbols begin to approach the cross-correlation levels of the ISDP symbols, but still have $\approx$ 10 dB greater peak cross-correlation than the ISDP symbols. Note that the ISDP symbols only reduce their average cross-correlation by $\approx$ 2 dB compared to the $m = N/2$ case shown in Figure 3. Therefore, the ISDP symbols may be designed to possess significant spectral overlap with the radar, providing more degrees of freedom with which to embed information, while still maintaining low cross-correlation.

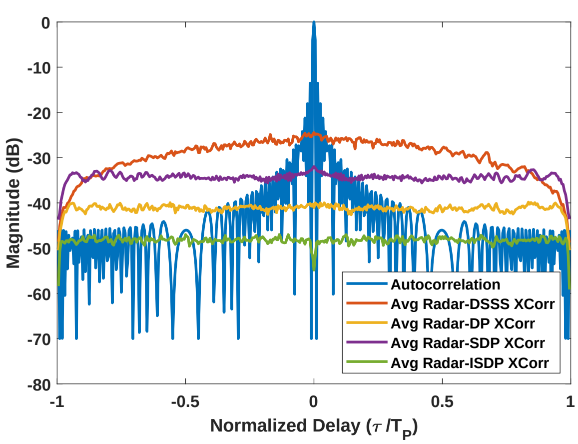

Fig. 4. Radar matched filter output for $m = N$.

Note that Figures 3 and 4 only show the cross-correlation response of the radar and the communication symbols. However, as the communication symbols by definition will change from pulse-to-pulse, the output of pulse-Doppler processing the communication symbols will not be coherent. The Doppler leakage caused by the presence of the communication symbols is seen by comparing Figures 5 and 6. From visual inspection, the Doppler leakage due to varying communication symbols appears to be uniform. Due to page limits, further analysis is omitted here. But due to the use of the complex Gaussian spreading sequences, the output of pulse-Doppler processing the communication symbols is likewise complex Gaussian distributed. As such, the presence of the communication symbols may be treated as simple interference for the purposes of CFAR processing, as opposed to traditional communication waveforms that impact the CFAR processing even in negative INR regimes [4], [5].

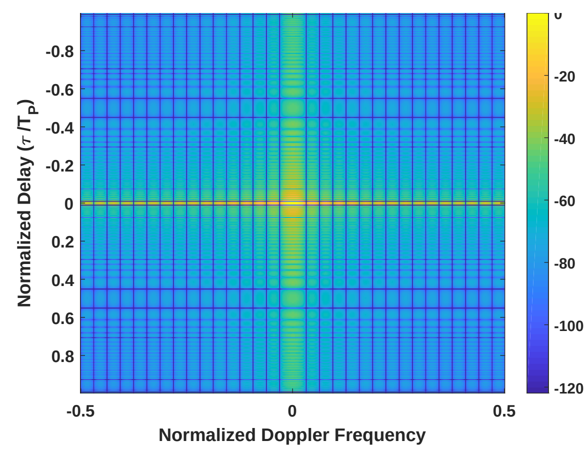

Fig. 5. Range Doppler map generated with 32 pulses and no communications symbols present

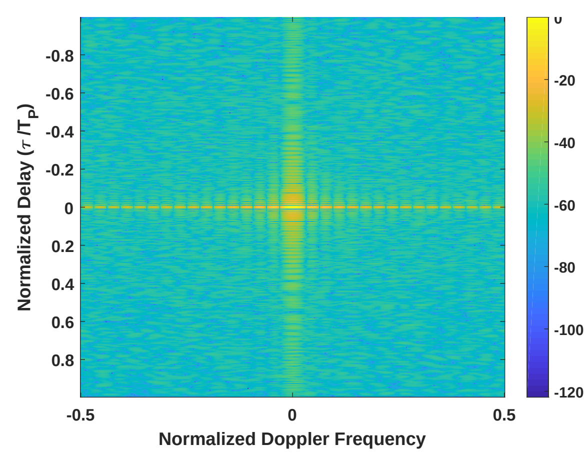

Fig. 6. Range Doppler map generated with 32 pulses and ISDP communications symbols present

C. Communication Performance

The symbol error rate (SER) for the communication symbols is shown in Figures 7 and 8 for an interference level of SIR = -5 dB, where the SIR is measured as the *input* SIR of the communication symbol and radar waveform, specifically. The SNR is measured as the *output* SNR after matched filtering. To bound performance, it is assumed here that the communication receiver is perfectly synchronized. Note that there is an $\approx$ 2 dB SER penalty for using $m = N/2$ rather than $m = N$, with a corresponding increase in symbol density of 50% (i.e. $m = [N/2, N]$ corresponds to $K = [3N/2, N]$, respectively). As the SER performance of the ISDP symbols is comparable to the DP and SDP sybmols, the ISDP symbols may share some of the resiliency to multipath observed in the DP and SDP symbol designs [14]–[17], and this will be addressed in future work. Due to the assumptions in equations (7)-(8), the matched filter was used in this analysis. As a baseline, future work will examine the use of the decorrelating filter used in [14], [15].

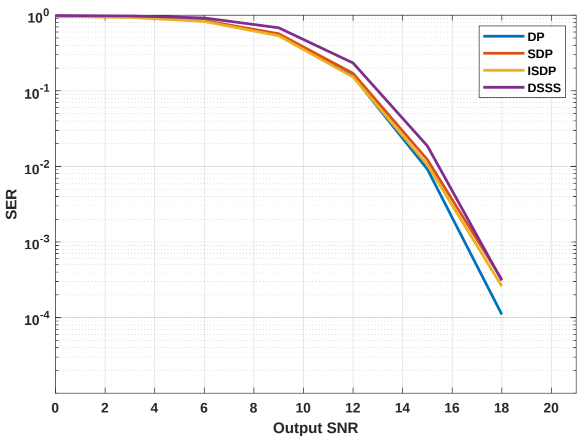

Fig. 7. SER for symbols with $m = N/2$, SIR = -5 dB.

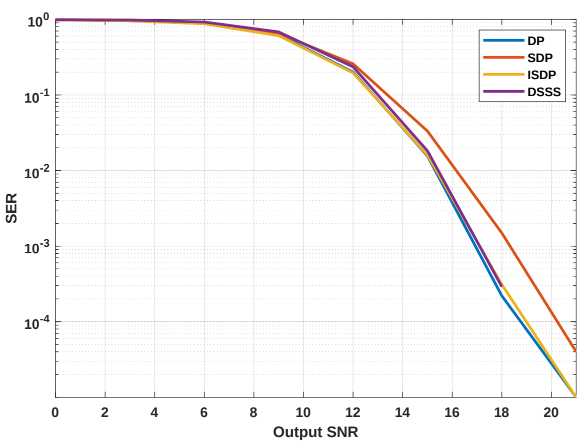

Fig. 8. SER for symbols with $m = N$, SIR = -5 dB.

V. Conclusion

We have presented an new communication symbol design that reduces the interference at the output of radar signal processing by $10 - 45$ dB while maintaining a comparable symbol error rate relative to previously presented designs. The interference to radar operation was examined from both a cross-correlation perspective as well as at the output of Doppler processing.

However, there are numerous open questions still to be answered with this symbol design, the least of which are synchronization, equalization, and sensitivity of the polyphase codes to bit quantization and hardware distortion, and an extension to multi-user communications. Also, the spectral containment of the proposed waveform *away* from the radar has yet to be examined.

Acknowledgment

This work was supported by a subcontract with Matrix Research, Inc. for research sponsored by the Air Force Research Laboratory under Prime Contract #FA8650-14-D-1722.

References

[1] A. Aubry, A. De Maio, M. Piezzo, and A. Farina, "Radar waveform design in a spectrally crowded environment via nonconvex quadratic optimization," *IEEE Transactions on Aerospace and Electronic Systems*, vol. 50, no. 2, pp. 1138–1152, Apr. 2014.

[2] A. Aubry, V. Carotenuto, and A. D. Maio, "Forcing multiple spectral compatibility constraints in radar waveforms," *IEEE Signal Processing Letters*, vol. 23, no. 4, pp. 483–487, Apr. 2016.

[3] F. Hessar and S. Roy, "Spectrum sharing between a surveillance radar and secondary wi-fi networks," *IEEE Transactions on Aerospace and Electronic Systems*, vol. 52, no. 3, pp. 1434–1448, Jun. 2016.

[4] F. Sanders, R. Sole, B. Bedford, D. Franc, and T. Pawlowitz, "Effects of rf interference on radar receivers, ntia report tr-06-444," *US Department of Commerce, Tech. Rep*, 2006.

[5] D. P. Zilz and M. R. Bell, "Statistical modeling of wireless communications interference and its effects on adaptive-threshold radar detection," *IEEE Transactions on Aerospace and Electronic Systems*, vol. 54, no. 2, pp. 890–911, Apr. 2018.

[6] M. L. Parmentar and R. A. Romero, "Opportunistic techniques to inject OFDM subcarriers into navigational radar spectral guard bands and mainlobe for spectrum sharing," in *Proc. IEEE Radar Conf. (RadarConf)*, Apr. 2019, pp. 1–6.

[7] T. F. Settle, M. L. Picciolo, and J. S. Goldstein, "Environmentally-shaped colored spreading sequences for robust wireless communications," in *Proc. Int. Waveform Diversity and Design Conf*, Aug. 2010, pp. 000 040–000 044.

[8] S. D. Blunt and J. G. Metcalf, "Estimating temporal multipath via spatial selectivity: Building environmental knowledge into waveform design for radar-embedded communications," in *Proc. Int. Conf. Electromagnetics in Advanced Applications*, Sep. 2009, pp. 513–516.

[9] ——, "Using time reversal of multipath for intra-pulse radar-embedded communications," in *Proc. Int. Waveform Diversity and Design Conf*, Aug. 2010, pp. 000 155–000 158.

[10] S. D. Blunt and C. R. Biggs, "Practical considerations for intra-pulse radar-embedded communications," in *Proc. Int. Waveform Diversity and Design Conf*, Feb. 2009, pp. 244–248.

[11] S. D. Blunt, J. Stiles, C. Allen, D. Deavours, and E. Perrins, "Diversity aspects of radar-embedded communications," in *Proc. Int. Conf. Electromagnetics in Advanced Applications*, Sep. 2007, pp. 439–442.

[12] S. D. Blunt and P. Yantham, "Waveform design for radar-embedded communications," in *Proc. Int. Waveform Diversity and Design Conf*, Jun. 2007, pp. 214–218.

[13] J. Metcalf, S. Blunt, and E. Perrins, "Detector design and intercept metrics for intra-pulse radar-embedded communications," in *Proc. - MILCOM 2011 Military Communications Conf*, Nov. 2011, pp. 188–192.

[14] S. D. Blunt, J. G. Metcalf, C. R. Biggs, and E. Perrins, "Performance characteristics and metrics for intra-pulse radar-embedded communication," *IEEE Journal on Selected Areas in Communications*, vol. 29, no. 10, pp. 2057–2066, Dec. 2011.

[15] J. G. Metcalf, C. Sahin, S. D. Blunt, and M. Rangaswamy, "Analysis of symbol-design strategies for intrapulse radar-embedded communications," *IEEE Transactions on Aerospace and Electronic Systems*, vol. 51, no. 4, pp. 2914–2931, Oct. 2015.

[16] J. Metcalf and C. Sahin, "Embedding communication symbols in radar clutter on an intra-pulse basis," in *Radar & Communication Spectrum Sharing*, S. Blunt and E. Perrins, Eds. IET, 2018, ch. 21.

[17] S. D. Blunt, P. Yatham, and J. Stiles, "Intrapulse radar-embedded communications," *IEEE Transactions on Aerospace and Electronic Systems*, vol. 46, no. 3, pp. 1185–1200, Jul. 2010.